Charge-density waves and many-body effects in x-ray photoelectron spectroscopy of layer-structure chalcogenides

G. K. Wertheim, F. J. DiSalvo, and S. Chiang*
Bell Laboratories, Murray Hill, New Jersey 07974
(Received 10 November 1975)

Comparison of x-ray photoemission spectra of semiconducting and metallic layered transition-metal dichalcogenides clearly exhibits the role of many-electron screening in these largely two-dimensional conductors. The effect of the charge-density wave (CDW) has been observed in 1 T-TaS_2 and $TaSe_2$ as a perturbation of the initial-state $4f$ electron binding energy. In the commensurate CDW state these levels show a resolved splitting; in the quasicommensurate and incommensurate CDW states they show broadening of magnitude comparable to this splitting. The sign and amplitude of the CDW is determined from a comparison of these observations with a theoretical model.

The discovery of charge-density waves[1-3] (CDW) in the d^1 layer compounds by electron diffraction has given experimental confirmation of a hitherto purely theoretical concept. The size and orientation of the CDW superlattice was determined for TaS_2, $TaSe_2$, and $NbSe_2$, and the nature of the phase transitions in the compounds elucidated. These measurements did not, however, determine either the magnitude or the sign of the wave. By x-ray photoelectron spectroscopy (XPS) it now seems possible to determine these characteristics from cation core-level spectra.

Earlier XPS work, concerned chiefly with the valence-band density of states,[4,5] had turned up unusual core-level spectra in some of these compounds which can now be related to the CDW. The two compounds for which data are shown in Fig. 1 illustrate this point. They are isostructural, and the two cations are adjacent in the periodic table, having zero and one d electrons, respectively, in the four-valent state. The earlier density of states work confirmed quite clearly that HfS_2 is a semiconductor while TaS_2 is a metal. At that time the relevance of this observation to the shape of the core-level spectra was not appreciated. Most puzzling was the fact that the Ta $4f$ spectrum is broad and asymmetrical while that of the Hf is well behaved, i.e., compatible with an instrumentally broadened Lorentzian. The excess width cannot be attributed to lifetime since other Ta compounds, e.g., Ta_2O_5, have $4f$ lines similar to those of HfS_2. Phonon broadening[6-8] cannot be invoked because it is important only in good insulators. If it were relevant to this problem it should be much more important in semiconducting HfS_2 than in metallic TaS_2. A less apparent, though significant difference between the two materials can be found in the S $2p$ spectra. Those of HfS_2 are essentially symmetrical while those of TaS_2 tail out toward greater binding energy. As we shall show below, all these observations are now well understood. Some of the unusual behavior of the metallic compound arises from many-body screening effects in photoemission and others from the CDW. Detailed analysis leads to a determination of the sign and amplitude of the CDW.

The materials used in the present investigation were grown by the technique previously described.[2] Single-crystal samples, typically 3×4 mm^2, were mounted with indium or conducting epoxy on a gold-plated copper sample holder, and were cleaved in a dry nitrogen atmosphere in a chamber attached to the spectrometer.[9] The latter is a HP 5950A operating with monochromatized Al $K\alpha$ radiation. The low sticking coefficient on a high-quality surface of these materials leads to negligible oxygen and carbon contamination. The carbon is, however, difficult to determine quantitatively in Se compounds because a Se Auger line nearly coincides with the carbon $1s$ position. In the 10^{-9} Torr vacuum of the spectrometer these samples generally remained uncontaminated during the 24 h needed to obtain core and valence electron spectra. Data were taken at room temperature unless otherwise noted.

We begin the more detailed analysis by returning to the $4f$ spectra of HfS_2. Superposed on the data points in Fig. 1 is a solid line computed by convoluting a Lorentzian, representing the lifetime width, with a two parameter representation of our resolution function.[10] The theoretical 3:4 amplitude ratio was used for the two spin-orbit components. A lifetime width of 0.23 eV full width at half-maximum and a spin-orbit splitting of 1.71 eV were used. The quality of the fit is not sufficiently good to rule out phonon broadening entirely, but it can at most make a small contribution to the width. The higher background level on the left may be attributed to degraded electrons. These make only a small contribution to the spec-

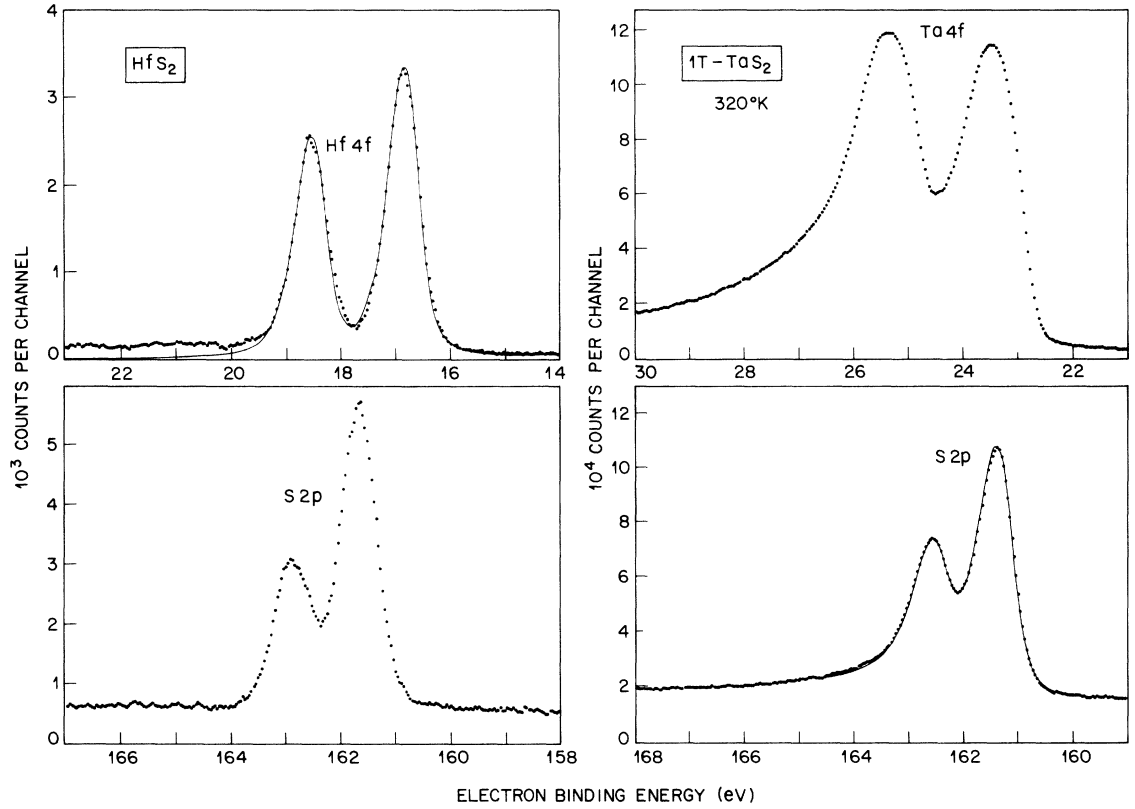

FIG. 1. Comparison between the XPS lineshapes of semiconducting HfS_2 and metallic $1T$-TaS_2. Uncorrected data are shown. A symmetrical doublet has been superposed on the Hf $4f$ spectrum, and one based on Eq. (1) on the S $2p$ lines of TaS_2.

trum. The S $2p$ spectrum has quite similar characteristics. This easily understood behavior is characteristic of all the semiconducting compounds we have examined; see also Figs. 2(a) and 2(b) which show data for two additional layer-structure compounds. The absence of phonon broadening indicates that electronic screening is sufficiently fast to prevent the generation of phonons by the sudden creation of the hole. On the other hand, the density of states at the Fermi energy is sufficiently low so that many-body effects do not take up an appreciable energy.

These many-electron screening effects, long predicted theoretically,[11] have only recently been demonstrated to be quantitatively present in XPS. Specifically it has been shown that the power-law singular shape obtained by Nozières and De Dominicis,[12,13] suitably modified to include lifetime effects,[14] provides a good description of XPS data over a range of many electron volts in noble, transition, and s-p metals.[15-17]

In the formulation due to Doniach and Sunjic[14] the following form is obtained for the line shape:

$$I(\epsilon) \propto \frac{\cos[\pi\alpha/2 + (1-\alpha)\arctan\epsilon/\gamma]}{(\epsilon^2+\gamma^2)^{(1-\alpha)/2}} , \qquad (1)$$

where α is a singularity index which ranges between 0 and $\frac{1}{2}$, ϵ the energy measured from the center of the unperturbed transition, and γ the half-width due to the lifetime of the core hole state created by photoemissions. It is readily verified that this function approaches the singular form[11,12] $1/\epsilon^{1-\alpha}$ for $-\epsilon/\gamma \gg 1$, and becomes Lorentzian as α approaches zero. More complicated effects appear only when there is a high density of states at E_F,[18] or when the width of the conduction band is unusually small.[19] In the simple cases the excitation of electrons across the Fermi surface during the photoemission process results in a line which tails out smoothly toward greater binding energy while retaining its Lorentzian character on the low-energy side.[20] The excitation of hole-electron pairs is simply another way of describing the screening response of the conduction electrons to the sudden creation of a localized potential, the core hole. From this point of view the process is described by the Friedel phase shifts δ_l, which also define the singularity index

$$\alpha = 2\sum_{l=0}^{\infty}(2l+1)\left(\frac{\delta_l}{\pi}\right)^2 . \qquad (2)$$

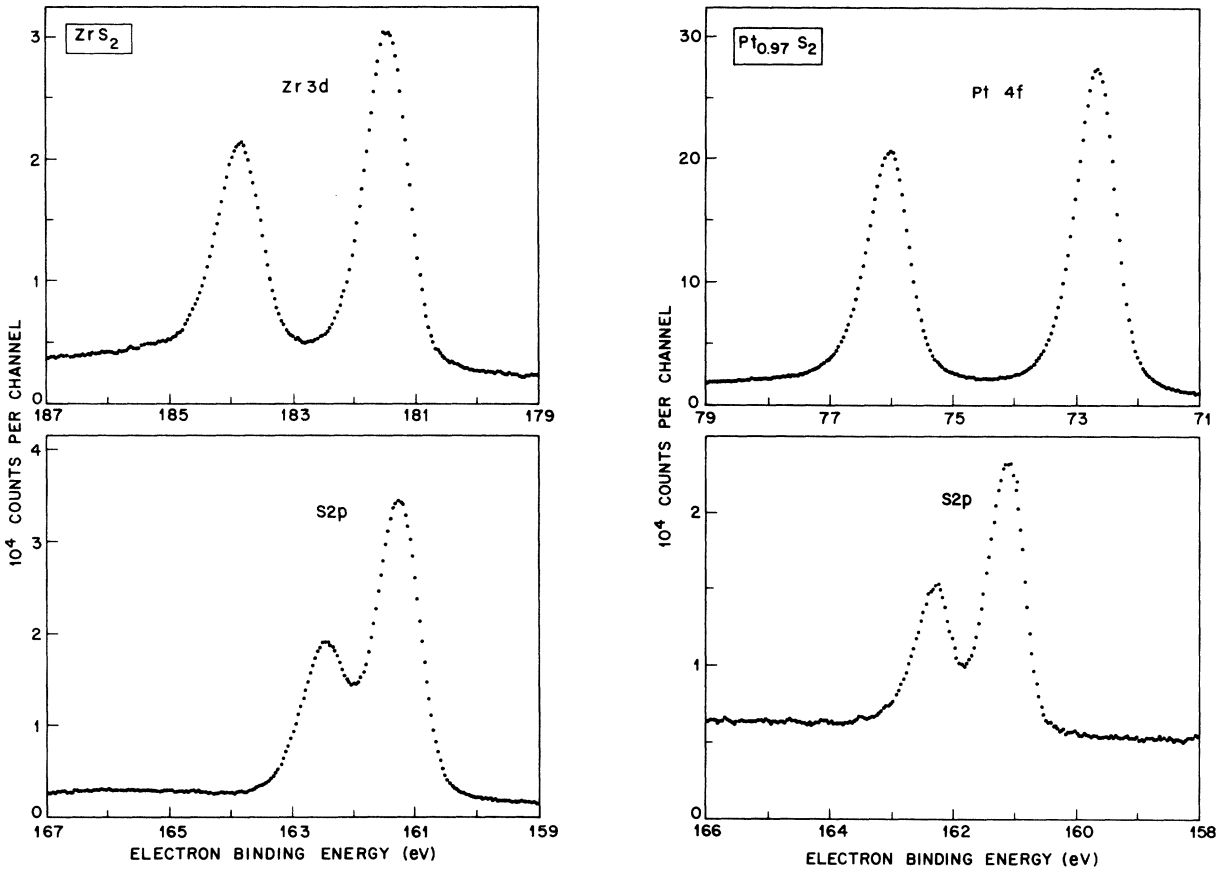

FIG. 2. Cation and anion XPS line shapes of two semiconducting layer structure compounds: (a) ZrS_2 (b) $Pt_{0.97}S_2$. The lines deviate only slightly from a symmetrical shape.

The phase shifts are, of course, constrained by the Friedel sum rule

$$Z = 2\sum_{l=0}^{\infty} \frac{(2l+1)\delta_l}{\pi} , \tag{3}$$

where Z is the charge to be screened, which is unity in photoemission. This phenomenon is certainly relevant to XPS in the metallic layer structure compounds, even though it is not clear to what extent the two-dimensional character of the conductivity will modify the behavior.

The S $2p$ data for TaS_2 in Fig. 1 provide a test case. The long tail, which one might earlier have ascribed to degraded electrons, is actually accounted for quite well by the many-body line shape with a lifetime width of 0.27 eV, a singularity index of 0.125, and a spin-orbit splitting of 1.20 eV. The apparent deviation of the intensity ratio from the theoretical value of 1:2 is not real, but arises from the tail of the $2p_{3/2}$ line which has appreciable amplitude under the $2p_{1/2}$ line (compare with the S $2p$ spectrum of HfS_2). The presence of many-body screening of the S $2p$ hole state indicates that there must be appreciable S $3p$ and $3d$ admixture into the Ta $5d$ conduction band.[21] [Screening by p electrons alone gives $\alpha = 0.167$, while d electrons alone give $\alpha = 0.10$, see Eqs. (2) and (3).] The attempt to account for the Ta $4f$ line using the many-body line shape leads to failure, largely because the data are not compatible with a lifetime shape (convoluted with the resolution function) on the low-energy side. The high-energy tail is, however, fairly well reproduced by the many-body theory.

This prompts us to examine the Ta $4f$ spectra of other materials. Those of the metal, cleaned by machining in vacuum, and of the nominally pentavalent compound $Fe_{1/3}Ta_{2/3}S_2$, produced by substituting low-spin divalent iron on the tantalum sites of TaS_2,[22] are shown in Fig. 3. The data for the metal have been analyzed to obtain the lifetime width of the $4f$ hole, yielding ~0.1 eV. The lifetime width in ionic compounds should, if anything, be smaller because there are fewer outer electrons available for Auger deexcitation.

At this point it becomes essential to examine

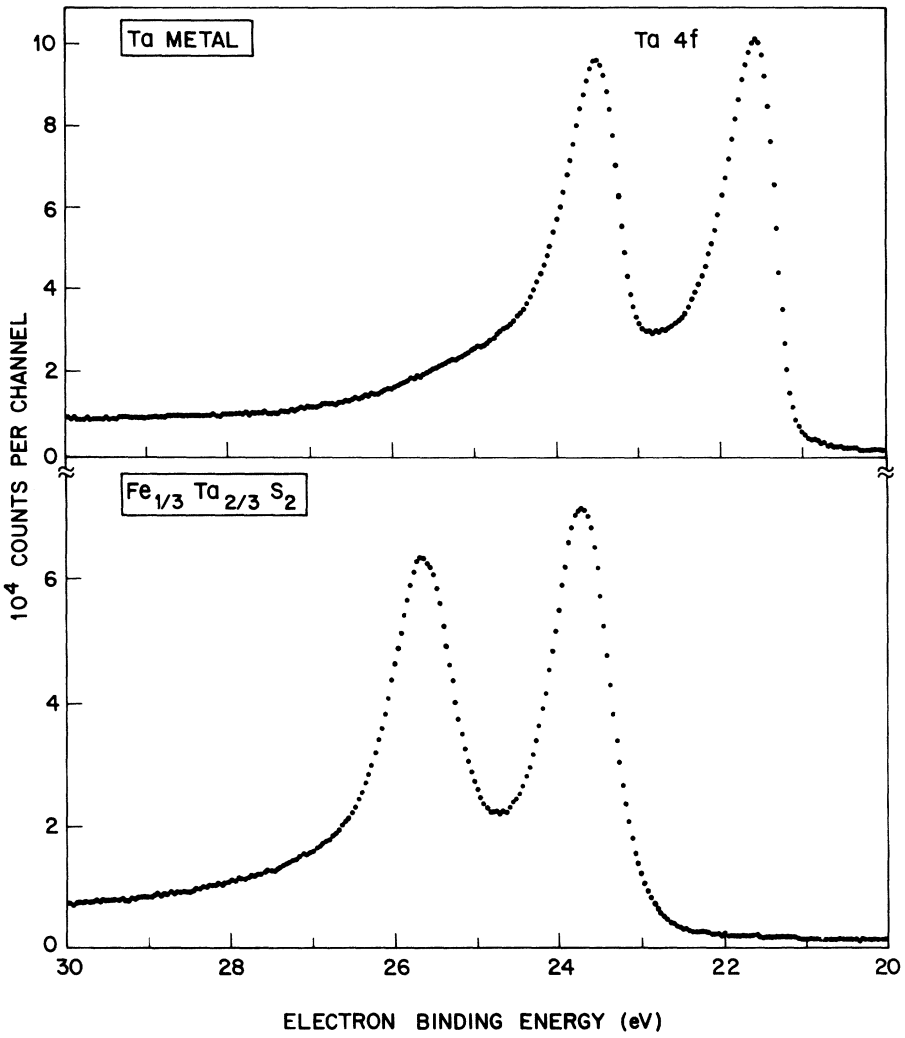

FIG. 3. Ta 4*f* spectra of metallic Ta cleaned by machining in vacuum, and of $Fe_{1/3}Ta_{2/3}S_2$ cleaved in an inert atmosphere. The former may have some surface contamination which contributes to the high-energy tail. The latter appears to be broadened by the random statistical cation neighbor environment.

whether the charge-density wave known to exist in $1T$-TaS_2 at room temperature could be responsible for the anomalous line shape. This wave is a spatial modulation of the occupancy of the Ta 5*d* derived conduction band and thus could, through local electrostatic effects and spatial modulation of the Madelung energy, shift core-level energies. In the following discussion we will focus on the electrostatic shifts due to changes in the occupancy of the *d* band at the Ta atom itself, under the assumption that the constancy of the average number of *d* electrons per metal atom will result in only small changes in the Madelung energy.

The characteristics of the CDW in $1T$-TaS_2 have been established in some detail from electron diffraction measurements.[1,2] The size and orientation of its unit cell in the commensurate state below ~180 K (T_d) is known, but its sign and amplitude are not. Between 180 and 350 K (T_d') the CDW is quasicommensurate, and above the latter temperature incommensurate.

The close relationship between the nature of the CDW and the XPS spectra[23] becomes apparent from the temperature-dependent data in Fig. 4. Note in particular the appearance of a resolved splitting of each of the lines of the spin-orbit doublet in the commensurate state (data at 140 K) and the slowly changing shape in the quasicommensurate range, indicated by the data at 220 and 320 K. The data in the incommensurate range at 380 K are more sharply peaked than those at lower temperature but are still incompatible with a lifetime shape.

Before we proceed to a more detailed discussion and analysis of these data, it is useful to obtain some independent confirmation of the association between the observed behavior and the CDW. The best evidence comes from similar data on the isostructural compound $1T$-$TaSe_2$ which has a commensurate CDW at room temperature. A similar

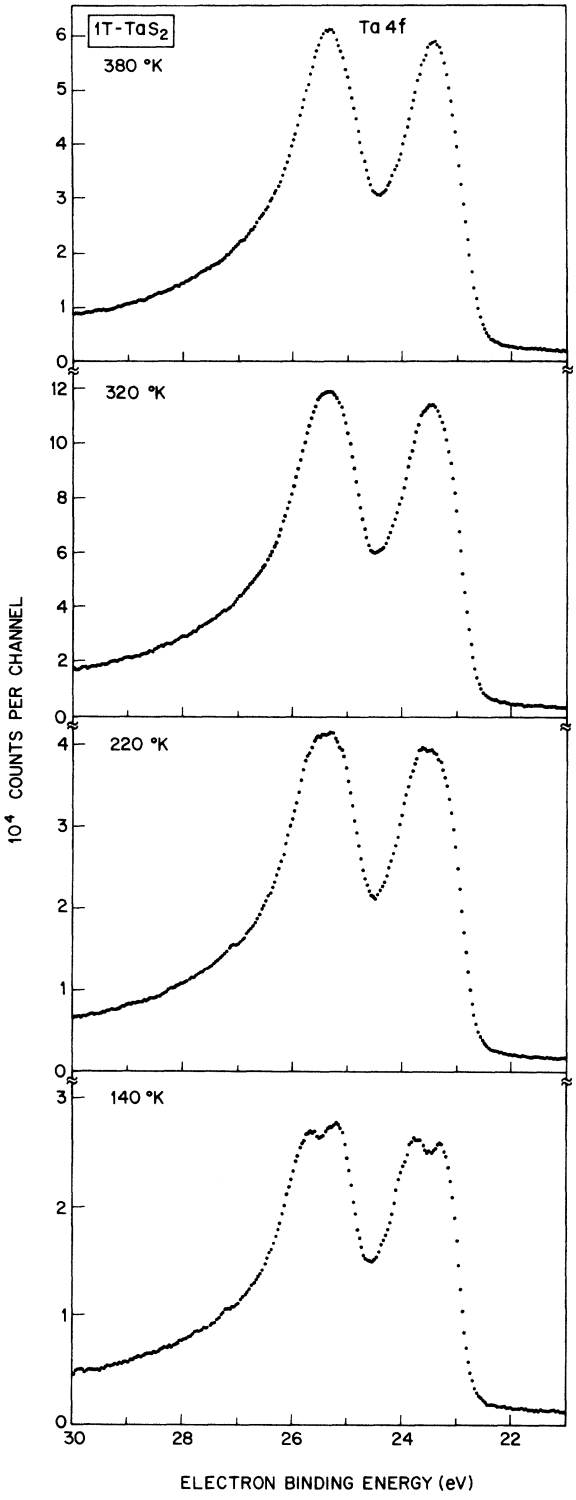

FIG. 4. Ta $4f$ spectra of $1T$-TaS_2 in three distinct regions of the CDW: at 380 K with an incommensurate CDW, at 320 and 220 K with a quasicommensurate CDW, and at 140 K with a commensurate CDW.

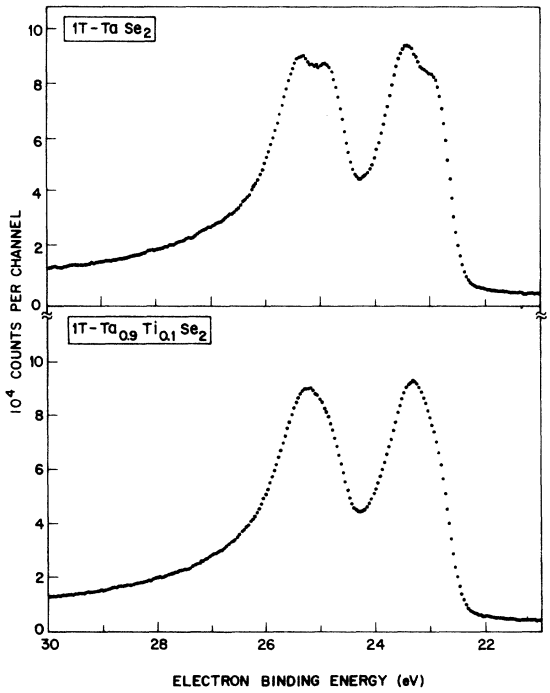

FIG. 5. Ta $4f$ spectra at room temperature of $1T$-$TaSe_2$ in which the CDW is commensurate and of $1T$-$Ta_{0.9}Ti_{0.1}Se_2$ in which it is incommensurate.

splitting of each of the spin-orbit components is again observed, together with a long tail toward greater binding energy, see the top of Fig. 5. Comparison with the data for metallic Ta, Fig. 3 shows that the rise on the low-energy side of $TaSe_2$ is comparable in slope to that of the metal, i.e., compatible with a lifetime shape convolved with the known resolution function. Further confirmation comes from the data for Ti-substituted $TaSe_2$,[24] shown in the bottom of Fig. 5. Quadrivalent Ti, which has no d electrons, produces a severe disturbance of the CDW, making it incommensurate. As expected, the resolved splitting of the spin-orbit components disappears, but the over-all width of the lines does not change significantly. The validity of the association of the width with the existence of the CDW can be further tested by comparison with the data for $Fe_{1/3}Ta_{2/3}S_2$, Fig. 3, in which the conduction band containing the CDW has been effectively emptied into lower-lying Fe d bands. As a result the compound loses its metallic conductivity and the CDW disappears. As expected, the XPS spectrum loses most of the many-body tail characteristic of metals, and the width, associated with the CDW, decreases. Some residual excess width does remain, however, presumably due to the electrostatic perturbations arising from the random occupancy of the cation neighbor environment by divalent iron and penta-

valent tantalum. The fact that the lines still exhibit a significant many-body tail indicates that the ~1-Ω cm resistivity is not indicative of true semiconductor behavior and that a finite electronic density of states remains at least a fraction of the Ta atom.

Further analysis depends on a detailed understanding of how the CDW affects the individual Ta atoms in the lattice. Here we depend on the model proposed in Ref. 2. Superposition of the Ta sites on the $\Phi = 90°$ CDW unit cell with an atom at the corner, see Fig. 6, shows that the 13 atoms associated with one cell fall into three categories with populations 6:6:1. The unique atom is at the corner of the cell. The charge-density perturbations associated with these sites are in a ratio of −1.15:0.65:3.00. Other ways of superposing the lattice on the CDW unit cell lead to a larger number of inequivalent sites. For example, if the corner is placed midway between three atoms, five inequivalent sites are obtained with 3:3:3:3:1 intensities, and charge-density modulation in a ratio of 2.0, 0.2, −0.75, −1.00, −1.50. The $\Phi = 120°$ CDW also leads to five inequivalent sites. An atom at the corner results in intensities of 1:3:3:3:3 and charge perturbations of 2.6, 0.75, 0.25, −0.2, −1.8, while the other case yields 3.3:1:3:3 and 1.55, 0.45, 0, −0.45, −1.55. It is immediately tempting to associate the two resolved components of each split spin-orbit line with the two high-population sites in the first $\Phi = 90°$ case, especially since more detailed analysis of the data clearly shows that they are made up dominantly of two components in each spin-orbit line. It turns out, however, that the attempt to synthesize the $TaSe_2$ 4*f* spectrum using three components with 6:6:1 intensities and a line shape chosen to reproduce the many-body tail is not successful; neither the shape of the tail nor that of the peak is well reproduced. It appears that this difficulty may be ascribed to the possibility that the individual components do not have the same many-body shape because the Fermi level lies in different parts of the band at the different sites. This results in distinct values of the singularity index which in turn causes the peak height to be different for lines with the same area. The magnitude of this phenomenon is, unfortunately, determined not only by α itself but also by an unknown cut-off energy,[20] making it difficult to introduce quantitatively into a simulation. We have, however, shown that by simply adjusting the amplitudes of the lines the 4*f* spectrum of $TaSe_2$ is well reproduced by the three site model. This phenomenon presumably also provides an explanation of the small differences between the spectra of TaS_2 and $TaSe_2$.

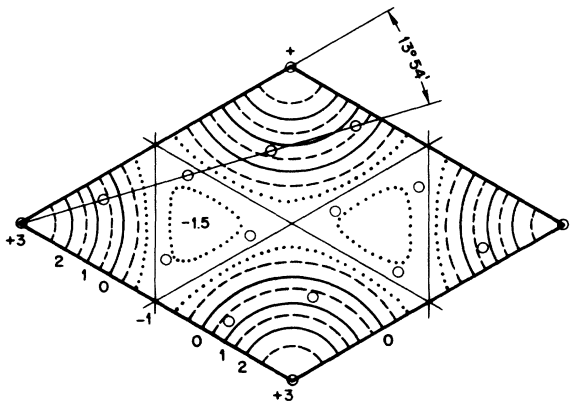

FIG. 6. $\Phi = 90°$ CDW unit cell (from Ref. 2) showing the atomic positions.

In the three site model, the shape at low energy requires that the low-intensity line lie at greater binding energy. This provides an initial determination of the sign of the CDW, because it requires that the *d*-band charge density be smallest at the unique site.

Calibration of the CDW amplitude is obtained from the shift of the 4*f* lines in compounds with known *d*-electron configuration. We restrict ourselves here to compounds with the same structure and covalency to avoid some of the worst ambiguities inherent in such a process. We use the line position in $Fe_{1/3}Ta_{2/3}S_2$ in which we assume the Ta atoms to be d^0. They are, however, in a lattice in which the average cation site is quadrivalent, just as in 1*T*-TaS_2, avoiding errors due to changes in the Madelung energy. For the other fixed point we use the estimated average position in TaS_2. Note, that this is not the centroid position of the asymmetric lines with their long tail, but generally a point on the low-energy side of the peak. The shift for the removal of the *d* electron of quadrivalent Ta is then 0.5 ± 0.1 eV. It is interesting, though perhaps more accidental than significant, that the shift between metallic Ta and Ta^{5+} is of similar magnitude, 0.4 eV/electrons (see Fig. 3).

This calibration, applied to the CDW, indicates that the two high-intensity sites which are separated by ~0.6 eV differ by more than one electron, and requires that the low-intensity site lose all of its *d*-electron charge. In fact, rigorous application of the results of this calibration to the harmonic CDW picture would require removal of more than the available charge. However, for a CDW whose amplitude is comparable to the average *d*-electron density a model using only one harmonic component cannot be expected to give an adequate representation. It is, of course, also possible that the calibration procedure is unreli-

able. If the shift were 1 eV/electron, the low-intensity site would just lose an entire electron in the harmonic model. The essential conclusion is that the CDW amplitude is comparable to the average d-electron density.

Since the CDW model works well in the commensurate range we will use it to analyze the behavior in the incommensurate range. When the CDW is not locked into the lattice the Ta atom positions will presumably fall at all points of the CDW with equal probability, i.e., they will sample the entire CDW uniformly. The expected $4f$ spectrum can then be constructed from the distribution function of the CDW amplitude under the assumption that charge density translates linearly into binding-energy shift, i.e., in terms of an electrostatic initial-state shift. Therefore we have reduced the CDW to a five-valued histogram into which we fold the line-shape function of Eq. (1), as well as our instrumental resolution function. The two spin-orbit components are generated as above. The energy scale of the histogram is determined from the comparison between data and the CDW in the commensurate range. The result of this calculation is shown in Fig. 7. On top we repeat the data in the incommensurate range. Directly below we show an attempt to represent the data without recourse to the CDW, by simply using a fictitiously short lifetime. The inadequacy of this approach is apparent on the low-energy side of the spectrum where the simulation is dominated by a Lorentzian tail not present in the data. The third panel shows the histogram result generated without adjustable parameters. It is generally successful, except with respect to the detailed shape of the peaks. This may be a result of the limited resolution of the histogram, or may again reflect the shortcomings of the single harmonic component model of the CDW. To test the assignment of the sign of the CDW we have also calculated the shape for a reversed histogram, see the bottom panel. The inferior result obtained clearly rules out an accumulation of negative charge at the corners of the CDW unit cell.

In the quasicommensurate range the line shapes are intermediate between the commensurate and incommensurate cases, (see the data at 220 and 320°K). This clearly indicates that the Ta atoms are no longer spatially sampling all parts of the CDW with equal probability, and supports the idea that there is in fact some type of temperature-dependent commensurate structure in this temperature range, possibly broken up into small phase domains.

The data in Fig. 4 also serve to illustrate that there is no simple, direct relationship between resistivity and the character of the many-body tail in

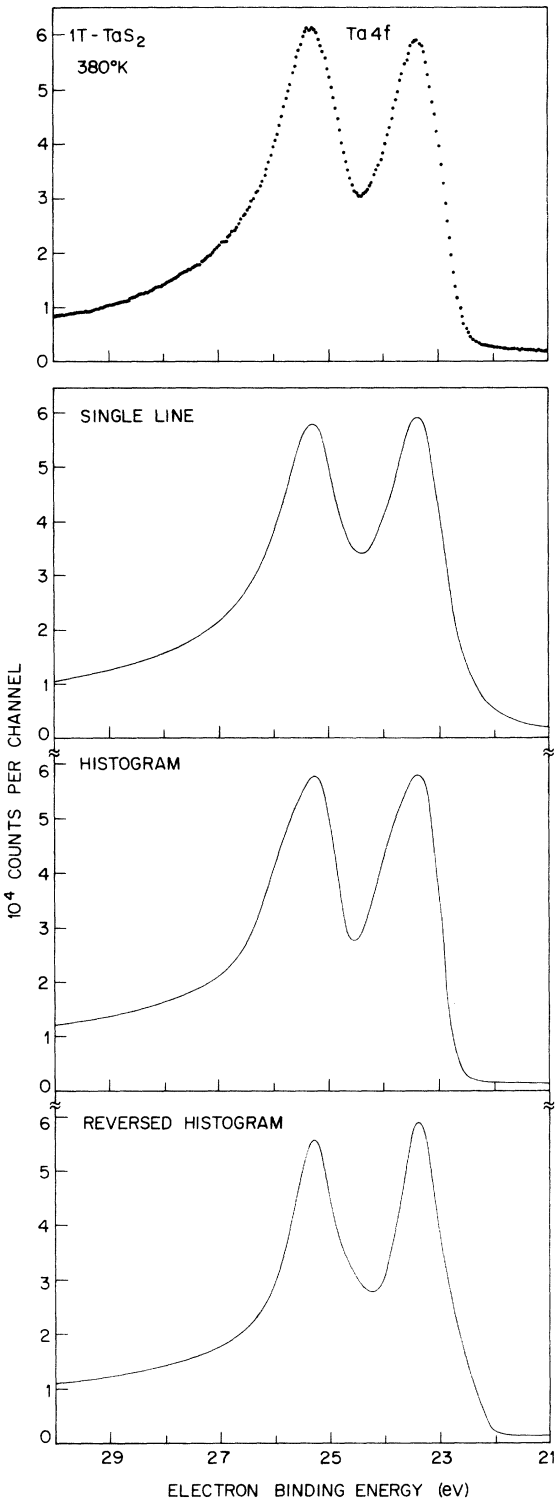

FIG. 7. Comparison of the spectrum of $1T$-TaS_2 in the incommensurate range with various simulations: (a) using a fictitiously large lifetime width, (b) based on the CDW histogram, and (c) based on the CDW histogram with reversed sign.

metallic materials. Over the range of temperature shown the resistivity changes by two orders of magnitude, but the tail remains largely invariant. Even the expression relating the singularity index to the square of the density of states[26] is in its simple form, valid only for metals with an *s*-like conduction band. Provided one is dealing with a material with a nonvanishing density of states at the Fermi energy, the best guide to the many-body behavior lies in Eqs. (2) and (3).

The finding that the CDW amplitude is so much larger in the Ta chalcogenides than in $NbSe_2$,[25] though perhaps unanticipated, is not really surprising. The fact that the CDW exists in the Ta compounds at 500 K while that in $NbSe_2$ forms only near 30 K is a good indication of the greater instability in the former materials. The tentative conclusion that the CDW actually leads to complete emptying of the *d* band for atoms on the corners of the CDW is perhaps simply an expression of the stability of the empty *d* shell which also makes so many common Ta compounds pentavalent.

ACKNOWLEDGMENTS

We are indebted to A. Wold for the sample of $Pt_{0.97}S_2$, and to J. A. Wilson for useful discussions throughout the course of this work.

---

*Present address: Harvard University, Leverett G-97, Cambridge, Mass. 02138.

[1]J. A. Wilson, F. J. DiSalvo, and S. Mahajan, Phys.Rev. Lett. 32, 882 (1974).

[2]J. A. Wilson, F. J. DiSalvo, and S. Mahajan, Adv. Phys. 24, 117 (1975), and references therein.

[3]C. B. Scruby, P. M. Williams, and G. S. Parry, Philos. Mag. 31, 225 (1975).

[4]G. K. Wertheim, F. J. DiSalvo, and D. N. E. Buchanan, Solid State Commun. 13, 1225 (1973).

[5]See also P. M. Williams and F. R. Shepherd, J. Phys. C 6, L36 (1973).

[6]U. Gelius, S. Svensson, H. Siegbahn, E. Basilier, A. Faxälv, and K. Siegbahn, Chem. Phys. Lett. 28, 1 (1974).

[7]P. H. Citrin, P. Eisenberger, and D. R. Hamann, Phys. Rev. Lett. 33, 965 (1974).

[8]J. A. D. Matthew and M. G. Davey, J. Phys. C 7, L335 (1974).

[9]The low sticking coefficient of nitrogen and residual atmospheric gases makes vacuum cleaving unnecessary.

[10]G. K. Wertheim, J. Electron. Spectrosc. 6, 239 (1975).

[11]G. D. Mahan, Phys. Rev. 163, 612 (1967).

[12]P. Nozières and C. T. DeDominicis, Phys. Rev. 178, 1097 (1969).

[13]See also K. D. Schotte and U. Schotte, Phys. Rev. 182, 479 (1969); and D. C. Langreth, *ibid.* 182, 973 (1969).

[14]S. Doniach and M. Sunjic, J. Phys. C 3, 285 (1970).

[15]G. K. Wertheim and S. Hüfner, Phys. Rev. Lett. 35, 53 (1975).

[16]S. Hüfner, G. K. Wertheim, and J. H. Wernick, Solid State Commun. 17, 417 (1975).

[17]P. Citrin, G. K. Wertheim, and Y. Baer, Phys. Rev. Lett. 35, 885 (1975).

[18]A. Kotani and Y. Toyozawa, J. Phys. Soc. Jpn. 37, 912 (1974).

[19]S. Chiang and G. K. Wertheim (unpublished).

[20]These theoretical line shapes are illustrated by Wertheim and Hüfner in J. Inorg. Nucl. Chem. (to be published).

[21]M. Campagna, G. K. Wertheim, H.R. Shanks, F. Zumsteg, and E. Banks, Phys. Rev. Lett. 34, 738 (1975).

[22]F. J. DiSalvo, M. Eibschütz, J. A. Wilson, and J. V. Waszczak, Bull. Am. Phys. Soc. 20, 290 (1975); M. Eibschütz and F. J. Di Salvo, Phys. Rev. Lett. 36, 104 (1976); F. J. Di Salvo, J. A. Wilson, and J. V. Waszczak, Phys. Rev. Lett. 36, 885 (1976).

[23]See also a brief report showing these data in Phys. Lett. A 54, 304 (1975).

[24]F. J. DiSalvo, J. A. Wilson, B. G. Bagley, and J. V. Waszczak, Phys. Rev. B 12, 2220 (1975).

[25]E. Ehrenfreund, A. C. Gossard, F. R. Gamble, and T. H. Geballe, J. Appl. Phys. 42, 1491 (1971).

[26]J. J. Hopfield, Comments Solid State Phys. 2, 40 (1969).